Template-Driven 3D Segmentation for Biomedical Images in Confocal Microscopy

Kai-Hsun Lee, Ying-Cheng Chen, and Yung-Chang Chen
Department of Electrical Engineering
National Tsing-Hua University, Hsinchu, Taiwan 300, R.O.C.
{kaishin, libra, ycchen}@benz.ee.nthu.edu.tw

Abstract

For biomedical research, high quality 3D visualization of particular anatomic structures is necessary for many applications. To achieve this, a variety of segmentation algorithms have been developed for different problems. For confocal microscopic images, the noise introduced during the specimen preparation process, such as the procedure of penetration or immunostaining, may cause confocal images to be of low contrast in some regions. This property will make 2D segmentation of some confocal images difficult and result in rugged surfaces in 3D visualization. In this paper, we present a specific algorithm for 3D segmentation of confocal images. It implements the 3D segmentation by a modified snake algorithm that is initialized by a registered template dataset. The modified snake algorithm segments each 2D slice separately, and then makes an iterative refinement to all slices by taking the local smoothness of surface into account. This will produce smoother segmentation results and eliminate the rugged surfaces in 3D visualization.

Keywords: segmentation, confocal microscopy, snake, template-driven

1 Introduction

In biomedical research, high quality 3D visualization of particular anatomic structures is necessary for diagnosis, surgical planning, biomedical inspection, structure understanding, etc. The raw data acquired from imaging modalities such as computed tomography (CT), magnetic resonance imaging (MRI) and confocal microscopy are conventionally consecutive 2D images. After these slices being stacked up, they will form a set of 3D volume data (an appropriate interpolation algorithm may be applied along the normal direction of 2D images to ensure an isometric volume data). We can obtain the structures of interest by segmenting these data, and then apply some rendering algorithm to present a 3D visualization for further applications. Consequently, it is a crucial problem to find a segmentation algorithm that can provide acceptable results for related applications.

Due to the nature of the problem of segmentation, a variety of specific algorithms have been developed. When the segmenting structures are stable over the population in study, atlas-guided approaches [1, 2, 3] are adequate. It finds the transformation relationship between the atlas and the target image by linear or nonlinear registration, and then warps the pre-segmented atlas to the target image to perform segmentation or labeling. For confocal microscopic images, the result of local nonlinear registration is no longer reliable because the properties of the acquired confocal images will vary from specimen to specimen (Noise is introduced during the specimen preparation process, such as the procedure of penetration or immunostaining). Since the confocal images are consecutive parallel 2D images, the easiest way to perform segmentation is to segment each 2D slice separately by appropriate 2D segmentation algorithms [4, 5, 6] and then 3D surface model can be reconstructed from these resulting parallel contours [7, 8]. Although this approach is simple, it will still encounter obstacles while dealing with confocal microscopic images. Due to the noise mentioned above, confocal images may be of low contrast and provide weak edges in some regions. Thus this approach can only promise the smoothness of 2D contours on the images, and may yield a nonsmooth surface along the normal direction of these parallel 2D images. Consequently, we present a template-driven 3D segmentation algorithm that combines the two methods mentioned above and make a modification to provide a solution for segmentation of confocal microscopic images.

This paper is organized as follows. Section 2 overviews the proposed algorithms. In Section 3 and 4 these algorithms will be presented in detail. The experimental results will be discussed in Section 5, and concluding remarks will be made in Section 6.

2 Overview of the Algorithm

The proposed algorithm is to segment particular anatomic structures from confocal microscopic image slices, i.e., image-stacks of parallel serial cross section. As shown in figure 1, the algorithm consists of three stages, preparation of template, registration of template and a modified snake algorithm.

The first stage is to prepare the template, or atlas, for the needs of the other two stages. The template comprises a set of raw confocal images, which is

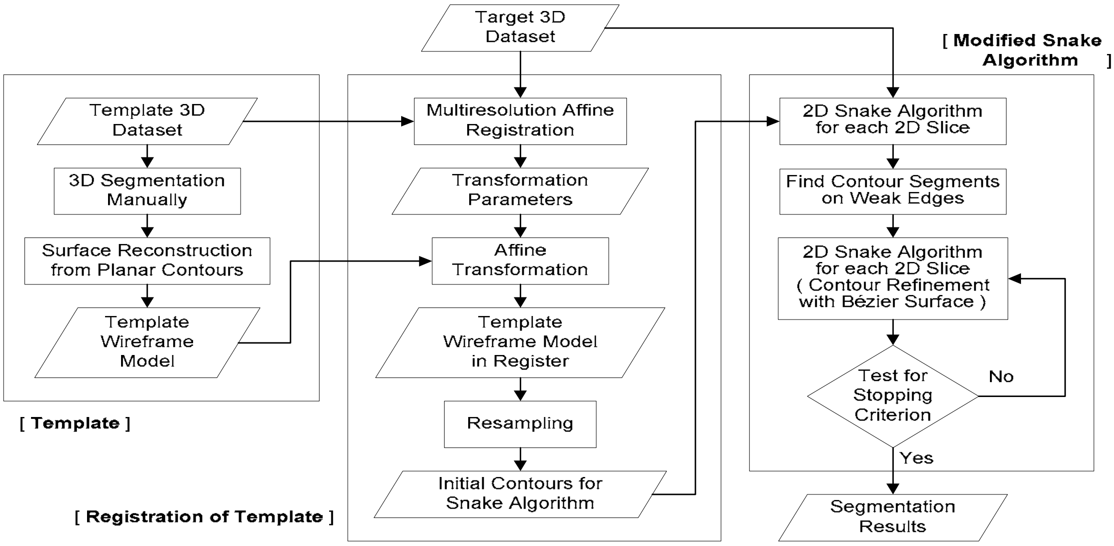

Figure 1: The system flowchart

called 3D dataset, and a wireframe model that describes the surface of pre-segmented particular anatomic structures. We can obtain the wireframe model by segmenting each raw slice manually and applying surface model reconstruction algorithms [7, 8]. Only one template is necessary for each population of study.

The second stage is to perform the registration of the template. The global affine transformation relationship between the template 3D dataset and the target 3D dataset can be determined with a multiresolution strategy. After warping the wireframe model with the same global transformation and resampling along the normal direction of each target slice with an appropriate interval, we can obtain a set of parallel contours on slices of the target 3D dataset. These contours can be interpreted as the suggested or estimated boundaries of segmentation results. They will be the initial contours for the snake algorithm in the next stage.

The final stage is to apply a modified snake algorithm. It takes the contours suggested by the template as the initial contours, and performs 2D snake algorithm to each slice in the target 3D dataset. After convergence, the resulting contours are examined to find the contour segments that are on weak edges. These contour segments will be applied with an additional external force that intends to maintain the local smoothness of surface. The modified 2D snake algorithm is performed to each slice again iteratively until convergence. Finally, we can obtain the segmentation results.

How to prepare the template is not the topic of this paper, and we will not go through it in detail. The other two stages will be discussed in the following sections.

3 Registration of Template

The registration procedure determines the global affine transformation relationship between the template 3D dataset and the target 3D dataset, and then provides a set of contours that suggest the boundaries of the particular anatomic structures to be segmented.

An affine transformation mapping from position $\mathbf{x}$ in the template dataset to position $\mathbf{y}$ in the target dataset is defined by

$$\begin{pmatrix} y_1 \\ y_2 \\ y_3 \\ 1 \end{pmatrix} = \begin{pmatrix} p_1 & p_4 & p_7 & p_{10} \\ p_2 & p_5 & p_8 & p_{11} \\ p_3 & p_6 & p_9 & p_{12} \\ 0 & 0 & 0 & 1 \end{pmatrix} \begin{pmatrix} x_1 \\ x_2 \\ x_3 \\ 1 \end{pmatrix} \quad \text{or } \mathbf{y} = \mathbf{Mx} \qquad (1)$$

The intensity difference between the target dataset and the transformed template at voxel *i* can be defined as

$$e_i(\mathbf{p}) = e_i(\mathbf{M}, p_{13}) = f(\mathbf{Mx}_i) - p_{13} g(\mathbf{x}_i) \qquad (2)$$

where p_{13} is the intensity scaling parameter, $f(\mathbf{x}_i)$ is the intensity of the target dataset at voxel *i* and $g(\mathbf{x}_i)$ is the intensity of the template dataset at voxel *i*. The objective function to be minimized is

$$\sum_i e_i^2(\mathbf{p}) = \sum_i \left(f(\mathbf{Mx}_i) - p_{13} g(\mathbf{x}_i) \right)^2 \qquad (3)$$

By applying the basic optimization algorithm [1], the iterative solution can be obtained

$$\mathbf{p}^{(n+1)} = \mathbf{p}^n - \left(\mathbf{A}^T \mathbf{A}\right)^{-1} \mathbf{A}^T \mathbf{b} \qquad (4)$$

where $\mathbf{A} = \begin{pmatrix} \frac{\partial e_1(\mathbf{p})}{\partial p_1} & \frac{\partial e_1(\mathbf{p})}{\partial p_2} & \cdots \\ \frac{\partial e_2(\mathbf{p})}{\partial p_1} & \frac{\partial e_2(\mathbf{p})}{\partial p_2} & \cdots \\ \vdots & \vdots & \ddots \end{pmatrix}$ and $\mathbf{b} = \begin{pmatrix} e_1(\mathbf{p}) \\ e_2(\mathbf{p}) \\ \vdots \end{pmatrix}$

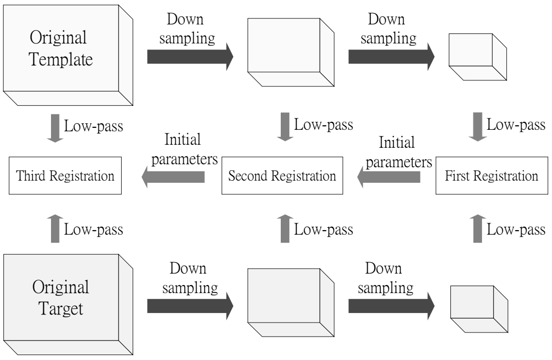

Figure 2: Multiresolution strategy

There is no guarantee that the global optimum will be achieved, since the solution might be trapped in a local minimum. A multiresolution strategy is adopted to alleviate this problem as shown in figure 2.

The obtained transformation parameters are applied to the transformation of all the vertices on the template wireframe model to bring the template wireframe model in register. After resampling the model along the normal direction of target slices with an appropriate interval, we can obtain a set of parallel contours on slices of the target 3D dataset. These contours will be the initial contours for the snake algorithm in the next section.

4 Modified Snake Algorithm

The first step to implement the modified snake algorithm is to perform a traditional snake algorithm to each slice of the target dataset. To improve the results of the snake algorithm, adequate initial contours are necessary and can be found in Section 3.

The traditional snake [6] is an energy-minimizing spline. Its energy function can be written as

$$E = \int_0^1 \left[E_{int}\left(v(s)\right) + E_{image}\left(v(s)\right) + E_{con}\left(v(s)\right) \right] ds \qquad (5)$$

where E_{int} is the internal energy of the contour due to bending, E_{image} is the potential function defined on the image plane, and E_{con} gives rise to the external constraint forces. For the proposed algorithm, E_{image} is defined by the magnitude of image gradient and E_{con} is implemented by the balloon model [4, 5] to reduce sensitivity to contour initialization.

After convergence of the 2D snake algorithm, the resulting contours are examined to find the contour segments that are on weak edges. If the local average of the image gradient magnitude at a control point on the snake is smaller than a threshold, the control point is referred to be on weak edges. An additional energy will be applied to these contour segments and the others remain original. To construct this additional energy field for a particular contour segment, we find the corresponding contour segments on adjacent and nearby slices by the contour matching algorithm [7] first. A Bézier surface [9] is estimated with these contour segments to yield a smooth surface locally. By intersecting the smooth surface with the slice which the particular contour segment is on, we can obtain a suggested contour segment that intends to maintain the local smoothness of surface. The additional energy field can be attained by applying a fast distance transformation algorithm [10] to the suggested contour segment. The position that is closer to the suggested contour segment will have lower energy. While minimizing the additional energy, a force will pull the particular contour segment toward the suggested contour segment.

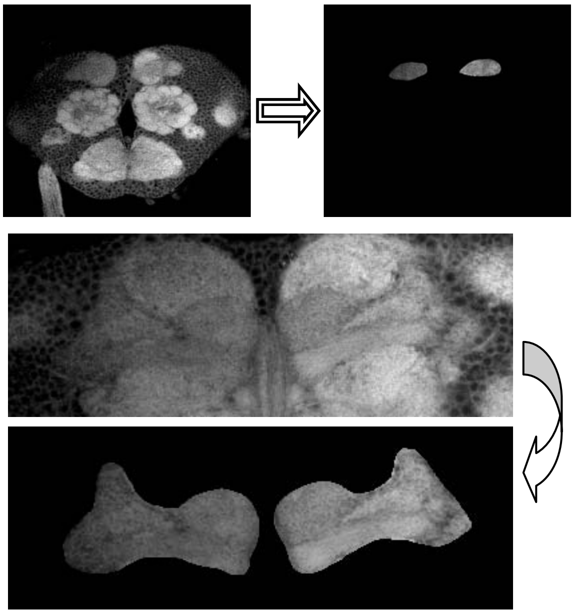

Figure 3: Confocal images and corresponding manually segmentation results

The process of contour refinement is repeated from slice to slice until the disparity between two successive cycles is smaller than a threshold or the iterations exceed a fixed number. Once the process is completed, the final segmentation results can be obtained.

5 Experimental Results

The confocal microscopic images used in this study are scans of *Drosophila* brains. What we are trying to segment from the raw data is the mushroom body, lobed neuropils that are involved in olfactory learning and memory, of a *Drosophila*. Two slices of original scanned images and their corresponding manual segmentation results can be found in figure 3 (some regions are of low contrast and have weak edges). The results of template registration can be found in figure 4. The template model provides more reasonable initial contours after registration (they are closer to the manual segmentation results). The result of the

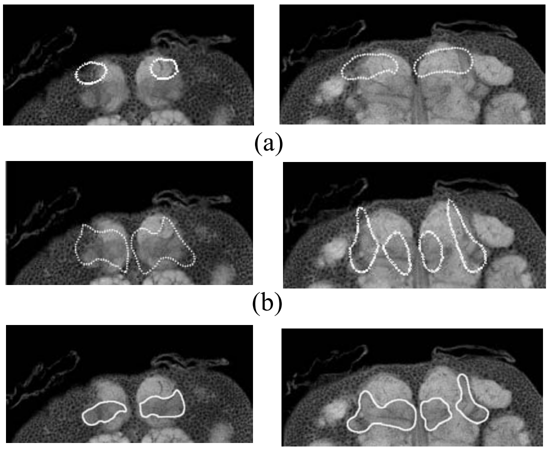

Figure 4: (a) suggested contours before registration (b) suggested contours after registration (c) manually segmentation results

modified snake algorithm is shown in figure 5. The manual segmentation results are provided by experts. They maintain local smoothness of surface manually in the segmentation procedure despite the degradation of images, and thus these manual segmentation results are referred to as "perfect segmentation". For slices without weak edges, the traditional snake is adequate for segmentation as shown in figure 5(a). By comparing figure 5(b) and 5(c), the segmentation result of modified snake is better than the traditional one for slices with weak edges. The result in figure 5(c) is closer to the manual segmentation result.

6 Conclusion

In this paper, we develop a specific algorithm for 3D segmentation of confocal images. A registration process of template generates suggested contours of particular anatomic structures to be segmented. And the modified snake algorithm is applied to the target dataset using the suggested contours as the initial contours. The results of traditional 2D snake are refined with a local estimation of smooth surfaces. After an iterative process, the final segmentation results can be obtained. The proposed algorithm provides a more efficient way to perform 3D segmentation than to do it manually. Also, it provides smoother segmented results that eliminate the effect introduced by the confocal microscopic noise that may cause confocal images to be of low contrast and produce weak edges in some regions.

Since the appropriate parameters of snake algorithm are different from case to case, a parameter training process should be performed in advance when dealing with each new population of study. For future works, if we can perform an automated analysis of the contour complexity for the template, we can determine the parameters automatically.

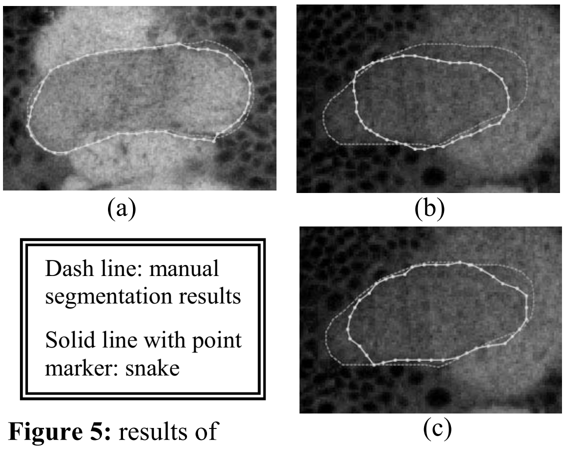

Dash line: manual segmentation results

Solid line with point marker: snake

Figure 5: results of (a)(b) traditional snake (c)modified snake (for the same slice used in (b))

7 References

[1] Toga, A.W., *Brain Warping*, Academic Press, San Diego (1999).

[2] Collins, D.L., Holmes, C.J., Peters, T.M., and Evans, A.C., "Automatic 3D model-based neuroanatomical segmentation," *Human Brain Mapping*, Vol. 3, pp. 190-208 (1995).

[3] Christensen, G.E., Joshi, S.C., and Miller, M.I., "Volumetric Transformation of Brain Anatomy," *IEEE Trans. on Medical Imaging*, Vol. 16, pp. 864-877 (1997).

[4] Wang, H., and Ghosh, K., "Boundary Finding with New Balloon Models", *Proceedings of the 20th Annual International Conference of the IEEE Engineering in Medicine and Biology Society*, Vol. 20, No 2, pp. 686-689 (1998).

[5] Cohen, L.D. and Cohen, I., "Finite-element methods for active contour models and balloons for 2D and 3D images," *IEEE Trans. on Pattern Analysis and Machine Intelligence*, Vol. 15, pp. 1131-1147 (1993).

[6] Kass, M., Witkin, A., and Terzopoulos, D., "Snakes: Active contour models," *International Journal of Computer Vision*, Vol. 1, pp. 321-331 (1988).

[7] Barequet, G., and Sharir, M., "Piecewise-linear interpolation between polygonal slices," *Computer Vision and Image Understanding*, Vol. 63, No. 2, pp. 251-272 (1996).

[8] Shih, M.Y., and Tseng, D.C., "Versatile surface model reconstruction from serial planar contours," *Proceedings of the 22nd Annual EMBS International Conference*, Vol. 4, pp. 2910-2913, 2000.

[9] Foley, J.D., van Dam, A., Feiner, S.K., and Hughes, J.F., *Computer Graphics: principles and practice*, 2nd Edition in C, Addison-Wesley, (1996).

[10] Meijster, A., Roerdink, J.B.T.M., and Hesselink, W.H., "A General Algorithm for Computing Distance Transforms in Linear Time". In: *Mathematical Morphology and its Applications to Image and Signal Processing*, J. Goutsias, L. Vincent and D. S. Bloomberg (eds.), Kluwer, pp. 331-340 (2000).